Aerosol and Air Quality Research, 15: 142–153, 2015

ISSN: 1680-8584 print / 2071-1409 online
doi: 10.4209/aaqr.2014.01.0014

On-Road Measurements of Ultrafine Particles and Associated Air Pollutants in a Densely Populated Area of Seoul, Korea

Kyung Hwan Kim[1], Daekwang Woo[1,2], Seung-Bok Lee[1], Gwi-Nam Bae[1*]

[1] *Center for Environment, Health and Welfare Research, Korea Institute of Science and Technology, Hwarangno 14-gil 5, Seongbuk-gu, Seoul 136-791, Korea*
[2] *Semiconductor & Memory Business, Samsung Electronics, San-16 Banwol-dong, Hwasungsi, Gyunggi-do 445-330, Korea*

ABSTRACT

Spatial distributions of ultrafine particles (UFPs; $6 < D_p < 560$ nm) and related gaseous and particulate pollutants were estimated from on-road measurements undertaken on busy roadways of Seoul, Korea, using a mobile laboratory (ML). The objectives of the study were to determine the spatial variations in UFP size distributions and concentrations of associated gaseous and particulate pollutants and to observe the relationships of UFP number concentrations with other pollutants on roadways in an urban area in Korea. The pollutants associated with diesel vehicles such as black carbon (BC) and particle-bound polycyclic aromatic hydrocarbons (PM-PAHs) exhibited a high determination coefficient ($r^2 = 0.65$), indicating the influence of diesel vehicles on emissions in the study area. Further supporting evidence for the influence of diesel vehicles on emissions was given by the higher determination coefficients of PM-PAHs and BC concentrations with larger size-classified particles, ranging from $60 < D_p < 220$ nm, than with total UFP number concentrations or smaller particles in the $6 < D_p < 60$ nm size range. Peak concentrations of measured pollutants were observed mostly at intersections, reflecting the relationships of transient driving modes (i.e., deceleration and acceleration) with emissions of UFPs, associated pollutants, and concentrated traffic volumes at such locations.

Keywords: On-road measurement; Particle number concentration; Black carbon (BC); Ultrafine particle; PM-PAHs.

INTROCUTION

Atmospheric ultrafine particles (UFPs; $D_p < 0.1$ μm) originating from natural sources and processes as well as from anthropogenic activities have attracted increasing interest in the last decade (Morawska *et al*., 2008). UFPs are important from the perspective of adverse health effects on humans as well as their subsequent growth into fine particles (FPs; $D_p < 2.5$ μm), which have the longest atmospheric residence time of all particulates and can be transported for long distances from the source area, contributing to regional-scale air pollution. Among the anthropogenic particulate matter (PM) sources, emissions of industrial combustion processes and traffic-related emissions account for the highest contributions of both UFPs and FPs (Schauer *et al*., 1996; Shi *et al*., 1999; Cass *et al*., 2000; EPA, 2000; Harrison *et al*., 2000; Hitchins *et al*., 2000). For traffic-related emissions, the greater part of the particle number concentration from vehicle exhaust is in the 20–130 nm size range for diesel engines (Kittelson, 1998; Morawska *et al*., 1998) and in the 20–60 nm for gasoline engines (Kittelson, 1998; Ristovski *et al*., 1998). PM emissions from internal combustion engines have traditionally been regulated solely on the basis of total PM mass emissions (Kittelson *et al*., 2004a). In response to such regulations, engines that emit much lower PM mass concentrations have been developed (Kittelson *et al*., 2004a). However, there is a concern that modern vehicles may emit smaller sized particles because of their advanced exhaust-gas management systems and factors such as driving conditions, which influence the emission of smaller particles.

Many studies have investigated the physical and chemical characteristics of UFPs or FPs near roadsides (Hitchins *et al*., 2000, Zhu *et al*., 2002a, b; Polidori *et al*., 2008; Buonanno *et al*., 2009; Hagler *et al*., 2009; Kim *et al*., 2011a, b). Studies have reported UFP concentration gradients near sources, including the rapid decrease in particle number concentrations with distance downwind of roadways (Hitchins *et al*., 2000, Zhu *et al*., 2002a, b; Polidori *et al*., 2008; Buonanno *et al*., 2009; Hagler *et al*., 2009; Kim *et al*., 2013). These stationary measurement studies provide useful data at roadsides but are less suitable for investigating the spatial distribution of UFPs and sharp gradients that characterize UFP concentrations on real roadways. Roadside and vehicle tail pipe exhaust measurements must be linked to understand the spatial

* Corresponding author.
Tel./Fax: +82-2-958-5676/+82-2-958-5805
E-mail address: gnbae@kist.re.kr

nature of UFPs, as well as differences in actual pollutant concentrations along roadways. Recent studies in various countries (China, Finland, Germany, Netherland, Switzerland, and United States) have developed mobile monitoring platforms using real-time instruments in attempts to estimate on-road air pollution concentrations together with spatial and temporal gradients of UFPs and related air pollutants (Bukowiecki *et al*., 2002a, b; Canagaratna *et al*., 2004; Kittelson *et al*., 2004a, b; Pirjola *et al*., 2004; Weijers *et al*., 2004; Schneider *et al*., 2008; Wang *et al*., 2009). Highways and arterial roads have been targeted for these measurements in both rural and urban areas. These studies provide information regarding UFP number concentrations with size distributions and levels of associated gaseous pollutants such as CO, CO_2, and NO_x under real-world conditions. However, most of these studies have been conducted in European countries or the United States. Few studies have been carried out using mobile monitoring platforms in Asian countries (Wang *et al*., 2009).

We carried out on-road measurements on busy roadways of Seoul, Korea, using a mobile laboratory (ML) to estimate air pollutants concentrations together with the spatial distributions of UFPs ($6 < D_p < 560$ nm in mobility diameter) and related gaseous and particulate pollutants. Our objectives were a) to provide UFP spatial variations and size distributions with associated gaseous and particulate pollutant concentrations and b) to observe the relationships of UFPs number concentrations with other pollutants on roadways in an urban area in Korea.

METHODS

Mobile Laboratory

We developed the ML for real-time on-road measurement in 2009 (Ministry of Environment, Republic of Korea). The ML enabled us to measure vehicle-related gaseous and particulate pollutants while driving. Sampling inlets were located at the top of the ML and consisted of a stainless steel pipe and Teflon tubing for particulate and gaseous pollutants, respectively. The sampling height was approximately 2 m above ground level as shown in Fig. 1.

The inlet for particulate monitoring was funnel-shaped with an inner entrance diameter of 10 mm. A stainless steel sampling line (48 mm inner diameter [I.D.] and 1.6 m length) was connected to the end of the funnel-shaped inlet and was also connected to a chamber (150 mm I.D.) inside the ML, labeled as A in Fig. 1. Air was pulled into the chamber at approximately 65 L/min by an inline pump located downstream of all sampling ports. The chamber contained five small inlet ports, which were connected to several instruments measuring aspects of particulate pollution as shown in Fig 1. All sample lines for particles were connected with conductive tubing. Teflon tubing was used for sampling gaseous pollutant and all sampling lines were kept very short (0.5–1 m) to minimize residence time and particle losses.

Measurement Equipment and Data Acquisition

Fig. 1 illustrates the ML instrument setup and Table 1 gives details of each instrument with the parameter measured and its time resolution. A fast mobility particle sizer (FMPS Model 3091, TSI Inc., Shoreview, MN, USA) was used to measure the particle number size distribution with the particle mobility diameter D_p at a flow rate of 10 L/min. The particles, which flow through a region of differing electrical fields, are repelled by the voltage from the central column. When the particles hit the outer cylinder, consisting of

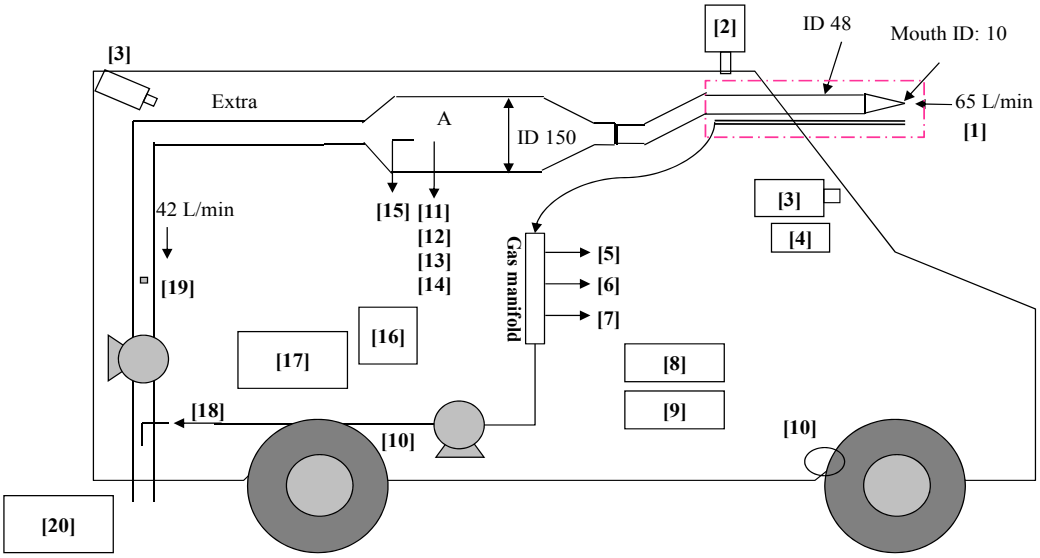

[1] Sampling inlets [2] Weather sensor [3] CCTV [4] GPS [5] CO/CO_2
[6] $NO/NO_2/NOx$ [7] NMHC [8] Inverter [9] Battery [10] Air suspension
[11] Condensation particle counter [12] Nanoparticle aerosol monitor [13] Particle-bound PAHs
[14] Aethalometer [15] Fast mobility particle sizer [16] DAQ and computer
[17] Power controller [18] Gas vent [19] Air velocity sensor [20] Power generator

Fig. 1. The mobile laboratory.

Table 1. Monitoring instruments used in the mobile laboratory.

Instrument	Parameter measured	Time resolution (s)
TSI Fast Mobility Particle Sizer (FMPS), model 3091	UFPs number, 5.6–560 nm (particles/cm^3)	1
AEROTRAK Nanoparticle Aerosol Monitor (NAM), model 9000	Particle surface area (Alveolar region; D_p < 1 μm) (μm^2/cm^3)	1
Aethalometer, model AE42 (Dual-wave length)	Black carbon mass (ng/m^3)	60
EcoChem PAS, model 2000 (Photoelectric aerosol sensor)	Particle-bound PAHs (ng/m^3)	6
Environmental S.A. CO analyzer, model CO12M (Infrared GFC CO analyzer)	CO, CO_2 (ppm)	3
Environmental S.A. NO_x analyzer, model AC32M (Chemiluminesence detector)	NO, NO_2, NO_x (ppb)	10

multiple cylindrical rings, the particle impact creates a current measured by electrometers (Weimer *et al*., 2009). The electrometer backgrounds were monitored and set to zero using particle-free air before each measurement. In the present study, UFPs size range was defined from 6 to 560 nm in mobility diameter.

The surface area of nanoparticle aerosols that deposit in the lung, as corresponding to the International Commission of Radiological Protection (ICRP) lung deposition curves for the alveolar (A) regions of the human respiratory tract, was monitored by a nanoparticle aerosol monitor (NAM Aerotrak 9000, TSI Inc.) equipped with a $PM_{1.0}$ cyclone for the removal of particles larger than 1.0 μm in aerodynamic diameter. Other measured pollutants included black carbon (BC), particle-bound PAHs, NO_x, and CO_2. The BC sample line was equipped with a $PM_{2.5}$ cyclone for the removal of particles larger than 2.5 μm in aerodynamic diameter, before utilizing a portable aethalometer (AE42 dual-wavelength, Magee Scientific, Berkeley, CA, USA), operating with quartz filter tape, illuminated by 370 and 880 nm wavelength light, with the allowable optical attenuation depth of the filter set to 1.25 (adjusted for 370 nm) at a flow rate of 5 L/min. Nitrogen oxides were measured with a NO_x analyzer, utilizing chemiluminescence (AC32M, Environmental S.A., Poissy, France). Carbon monoxide and carbon dioxide were measured with a non-dispersive infra-red (NDIR) analyzer (CO12M, Environmental S.A.). A photoelectric aerosol sensor (PM-PAHs; PAS 2000, EcoChem, League City, TX, USA) was used to monitor representative particulate PAHs. PM-PAHs with three or more rings were detected through the measurement of electrons emitted by organic molecules on particles irradiated by UV light. Further information regarding the principle of measurement by this technique is described in detail elsewhere (Burtscher, 1992; Dunbar *et al*., 2001). The air flow rate for the PAS 2000 sensor was set at 2.0 L/min and the lamp wavelength was fixed at 220 nm. As shown in Table 1, 6-s intervals, during which the lamp was off for 2 s and then on for 4 s, were used for measurements.

Driving Sections and Measurement

According to Statistics Korea (2011), about 18.4 million motor vehicles are registered in the country, with vehicles powered by gasoline, diesel, and liquefied petroleum gas (LPG) accounting for 49.7, 36.4, and 13.2% of the total, respectively. Of the total motor vehicles in Korea, 16.2% are registered in Seoul. Additional information about the traffic composition and volume is provided in Table S1 (Supplement). The Gangnam district is one of the most affluent areas of Seoul, with an area of 40 km^2 and a population of over 500,000. Several popular shopping and entertainment areas are located in the Gangnam district and an important business area runs east-west from Gangnam Station to Samseong Station. The Gangnam district is also surrounded by several expressways which could influence the air quality of the area. We chose this area for our study and drove the ML on fixed routes in the Gangnam district, as shown in Fig. 2.

The driving route covered the business, residential, shopping, and entertainment areas of the Gangnam district. We divided the driving route into five sections according to their characteristics, as shown in Fig. 2 and described in Table 2. Sections [1], [2], [3], [4], and [5] included business, residential, shopping, entertainment, and business with entertainment areas, respectively. The total driving distance was 16.31 km, with the distances covered in sections [1], [2], [3], [4], and [5] were 4.12, 3.74, 3.05, 2.19, and 3.21 km, respectively. To avoid the direct influence of vehicle exhaust plumes, we maintained a distance greater than 2–3 m from the nearest vehicle in front of the ML while driving. The measurements were conducted in the winter of 2011 and this study presents intensive and consecutive measurements from 11:19 to 16:40 hrs on 22 December 2011 (five measurements for each study area). Urban background concentrations at the roadside were measured when driving in section [2] (the location is indicated by the red square in Fig. 2). The blue circles, from A to F, indicate points where peaks of high pollutant concentrations were observed. These peaks are discussed later. Morning and evening rush hours were intentionally avoided to eliminate the influence of commuting (i.e., heavy traffic congestion) in the study area.

RESULTS AND DISCUSSION

Concentration Levels in the Different Driving Sections

Average vehicle speeds with corresponding meteorological information are shown in Table 3. The average vehicle speed was 16.5 ± 3.1 km/h and the wind predominantly blew

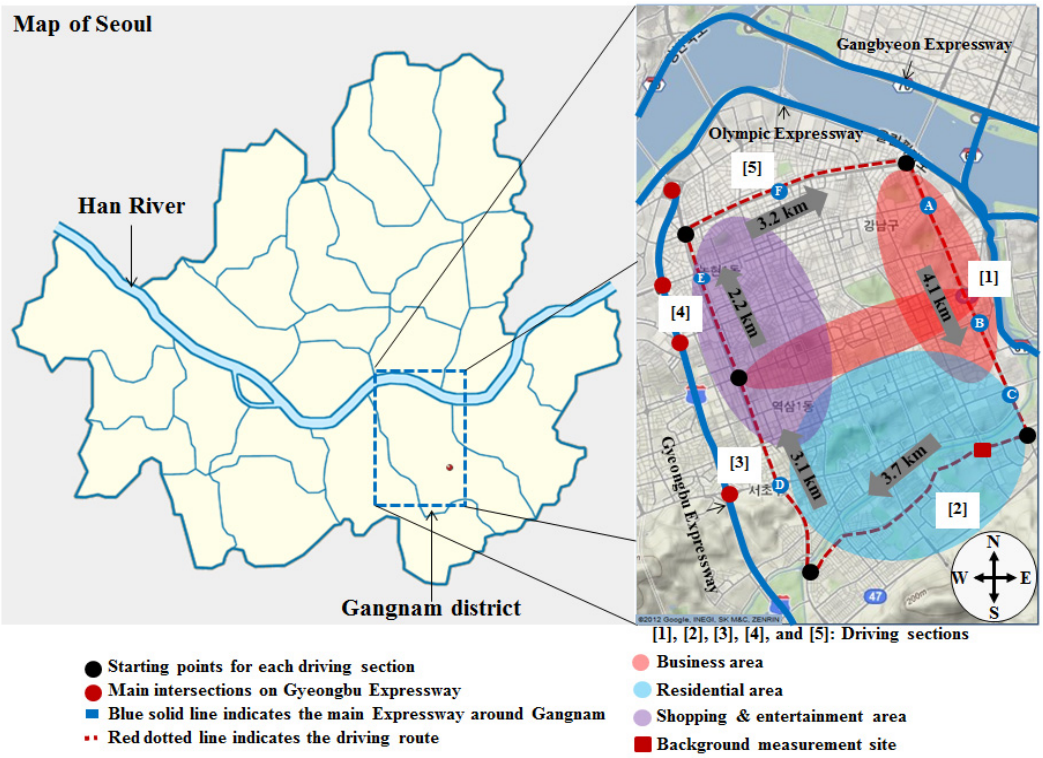

Fig. 2. Driving routes in Gangnam area, Seoul, Korea.

Table 2. Divided driving sections with distances and characteristics.

Sections	Average distance for each section (km)	Number of road lane	Characteristics of driving section
[1]	4.12 ± 0.04	14 → 10 → 8	Mainly business area
[2]	3.74 ± 0.09	4	Residential area
[3]	3.05 ± 0.08	4 → 8	Residential area + Shopping area
[4]	2.19 ± 0.03	8	Shopping and entertainment area
[5]	3.21 ± 0.04	10	Business, residential, shopping and entertainment mixed area

"±" indicates standard deviations of measured distances (n = 9).

from the west-northwest or northwest to southeast with an average speed of 3.2 ± 0.3 m/s during the five measurements. Table 4 presents the average concentrations of observed pollutants. The sample period was on a weekday and the measurements were repeated five times consecutively, to estimate the average concentrations.

The highest concentrations of pollutants, except for NO_x (NO and NO_2), were observed in section [1], and the lowest concentrations were found in section [2], as shown in Table 3. The winter monsoon typically blows from the northwest to southeast in Korea. The prevailing wind directions were northwest and north on the measurement day. These winds were assumed to have influenced the lower concentrations recorded in section [2] by reducing the direct influences from vehicles. In addition, dilution effects may have arisen from a stream that runs through section [2] in a northerly direction. Furthermore, a relatively smaller traffic volume due to fewer road lanes and the characteristics of section [2] (residential and school areas) could also have been factors in the lower pollutant concentrations in comparison to sections. Relatively low pollutant concentrations were expected in section [5] through which the Han River flows in a northward direction. However, pollutant concentrations in section [5] were similar to those in section [4]. Relatively wider road lanes (10 lanes) with large traffic volumes and high rise buildings, which may act as obstacles against horizontal mixing, could have influenced the observed pollutant concentrations in section [5].

Section [2] exhibited the smallest concentration variations, whereas section [4] showed the largest concentration variations for the five measurements (except for CO_2 concentrations). These temporal variations in pollutant concentrations reflect the mobility of vehicles travelling through the measurement areas. Despite the temporal variations for each driving section, generally high concentrations in section [1] and low concentrations in section [2] were observed throughout the measurement periods. This reflects the traffic volumes and the characteristics of these sections, i.e., a business area in section [1] and a residential area in section [2].

Table 3. Measurement periods and the average vehicle speed with meteorological information.

Order of measurements	Measurement periods	Traveled driving time (min)	Average vehicle speed (km/h)	Wind speed[a] (m/s)	Dominant wind direction[a]	Air temperature (°C)	Relative humidity (%)
1	11:19–12:16	57	17.3 ± 11.4	3.1 ± 0.4	NW	–3.1 ± 0.2	31.0 ± 0.3
2	12:16–13:02	46	21.4 ± 13.8	3.4 ± 0.6	WNW	–2.8 ± 0.2	30.6 ± 1.5
3	13:02–14:27	70	14.1 ± 12.4	3.2 ± 0.5	WNW	–2.6 ± 0.3	25.4 ± 1.6
4	14:27–15:30	63	15.6 ± 10.4	3.5 ± 0.3	WNW	–2.5 ± 0.2	25.7 ± 2.2
5	15:30–16:40	70	14.1 ± 11.4	2.7 ± 0.5	NW	–2.5 ± 0.3	27.8 ± 1.2
Average	-	61 ± 10	16.5 ± 3.1	3.2 ± 0.3	WNW	–2.7 ± 0.3	28.1 ± 2.6

[a] Data from "Air quality-Climate change information, Seoul" provided from a meteorological station located in Gangnam.

Table 4. Average pollutant concentrations on December 22, 2011.

Section	FMPS (#/cm^3)	BC (μg/m^3)	PM-PAHs (ng/m^3)	Surface area (μm^2/cm^3)	CO_2 (ppm)	NO (ppb)	NO_2 (ppb)	NO_x (ppb)	Number of data[a]
[1]	$1.1 \pm 0.2 \times 10^5$	9.0 ± 2.5	130.6 ± 2.4	74.7 ± 11.1	650.8 ± 15.2	150.8 ± 32.1	77.6 ± 18.6	209.2 ± 36.5	817 ± 147
[2]	$7.0 \pm 0.8 \times 10^4$	5.4 ± 0.5	53.9 ± 9.1	48.4 ± 6.3	605.0 ± 13.5	79.6 ± 13.6	45.4 ± 13.8	110.3 ± 28.3	700 ± 92
[3]	$9.3 \pm 0.9 \times 10^4$	6.0 ± 1.7	70.3 ± 23.4	54.3 ± 5.2	628.3 ± 12.1	159.7 ± 35.9	93.0 ± 23.9	240.9 ± 51.0	740 ± 171
[4]	$9.3 \pm 3.4 \times 10^4$	8.0 ± 3.7	94.5 ± 41.4	59.1 ± 12.9	631.8 ± 7.9	150.9 ± 44.2	76.6 ± 53.0	216.3 ± 93.1	677 ± 337
[5]	$7.9 \pm 1.2 \times 10^4$	7.0 ± 2.1	95.6 ± 24.9	59.3 ± 10.4	628.8 ± 16.6	97.4 ± 23.8	78.1 ± 26.5	166.4 ± 48.0	655 ± 50

" ± " indicates standard deviations of measured pollutants (n = 5).

"a" indicates the number of data based on 1 s data recording for each section (n = 5).

Correlations among Various Pollutants

Correlations were calculated to identify any relationships among pollutants (Fig. 3 and Table 5). Relatively high correlations were observed among PAHs, BC, and particle surface area, while UFP number concentrations showed moderate correlations with BC (r^2 = 0.32), CO_2 (r^2 = 0.33), and NO (r^2 = 0.42) and weak correlations with PAHs (r^2 = 0.20). The pollutants associated with diesel vehicles such as BC and PAHs showed high determination coefficients (r^2 = 0.65) indicating the influence of diesel vehicles in our study area. CO_2 was weakly or moderately correlated with other pollutants. Large quantities of CO_2 are emitted from all vehicles powered by fossil fuel and therefore a moderate correlation is not a surprising result. Similar moderate correlations (r^2 = 0.4–0.5) for CO_2 with other pollutants were reported by Westerdahl *et al*. (2005).

Westerdahl *et al*. (2005) also reported determination coefficients (r^2) above 0.7 for UFPs (0.007–1 μm) with BC, NO, and PM-PAHs. Although the monitoring instruments used in the current study were not identical to those used by Westerdahl *et al*. (2005), only moderate or weak correlations of UFPs with BC, PM-PAHs, and NO were obtained in our measurements. Therefore, we divided particle sizes into five groups [(a) $6 < D_p < 20$ nm, (b) $20 < D_p < 60$ nm, (c) $60 < D_p < 107$ nm, (d) $107 < D_p < 220$ nm, (e) $220 < D_p < 560$ nm)] and plotted these size categories against the other pollutants measured to clarify the relationship between fractional particle concentrations and air pollutants. No relationships were found for UFP number concentrations in the $220 < D_p < 560$ nm particle size range with measured pollutants.

Scatter plots of size-classified particles and PM-PAHs are shown in Figs. 4(a) and 4(b). The third of the five measurements, which included the roadside background measurement, was excluded from these plots owing to the different conditions at the background site. Unlike the poor correlations of total UFP number concentrations in Tables 5 and 6, size-classified particle groups (c) $60 < D_p < 107$ nm and (d) $107 < D_p < 220$ nm exhibited much higher determination coefficients with PM-PAHs and BC concentrations, whereas poor determination coefficients remained for the size-classified particle groups (a) $6 < D_p < 20$ nm and (b) $20 < D_p < 60$ nm. These results may reflect the relationship of relatively larger particles with PM-PAHs and BC.

Venkataraman and Friedlander (1994) investigated the size distributions of PAHs (PAHs with more than four rings) and elemental carbon (EC) in Los Angeles, CA, USA, and observed ambient PAH and EC size distributions with bimodal peaks in the 0.05–0.12 μm (mode I) and 0.5–1.0 μm (mode II) size ranges. They concluded that mode I particles were attributable to primary emissions from combustion sources whereas mode II particles were attributable to the accumulation of secondary reaction products on primary particles. Hence the lack of any relationship between UFP number concentrations in the $220 < D_p < 560$ nm particle size range with measured pollutants may have been a consequence of this bimodal characteristic of PAHs and BC. The poor correlations of the UFP number concentrations in the $6 < D_p < 60$ nm particle size range with other pollutants, can also be explained by the findings of Venkataraman and Friedlander (1994). The higher correlations of UFP number concentrations in the $60 < D_p < 220$ nm particle size range with PM-PAHs, BC, and particle surface area strongly reflect

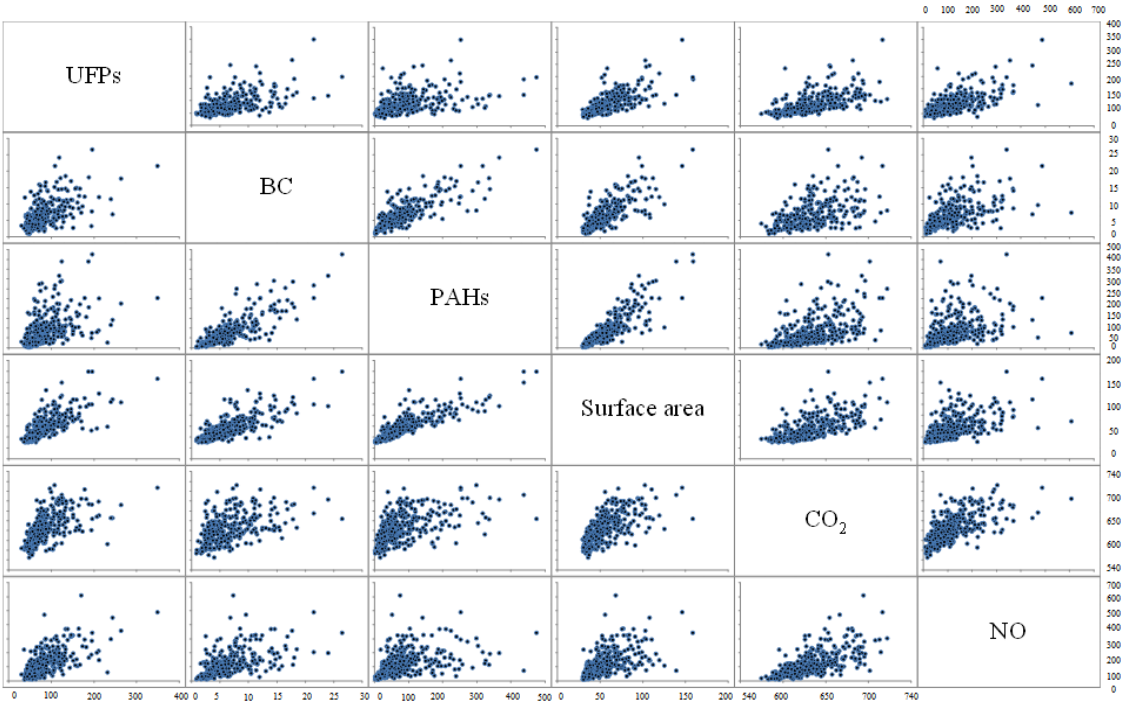

Fig. 3. Scatter plots from 60-s average concentrations on 22 December, 2011 (n = 324). Units are 1000-s of particles/cm^3 for UFPs, μm^2/cm^3 for surface area (NAM), μg/m^3 for BC, ng/m^3 for PAHs, ppb for NO, and ppm for CO_2 (range 540–740 ppm). Note x and y are identical for each pollutant.

Table 5. Pearson's correlation (r^2) for 60-s average concentrations on 22 December 2011 (n = 324, p < 0.001 except for the number in bold).

	UFPs	BC	PM-PAHs	Surface area	CO_2	NO
UFPs	1	0.32	0.20	0.51	0.33	0.42
BC		1	0.65	0.56	0.22	0.27
PM-PAHs			1	0.73	0.27	**0.16**
Surface area				1	0.40	0.28
CO_2					1	0.41
NO						1

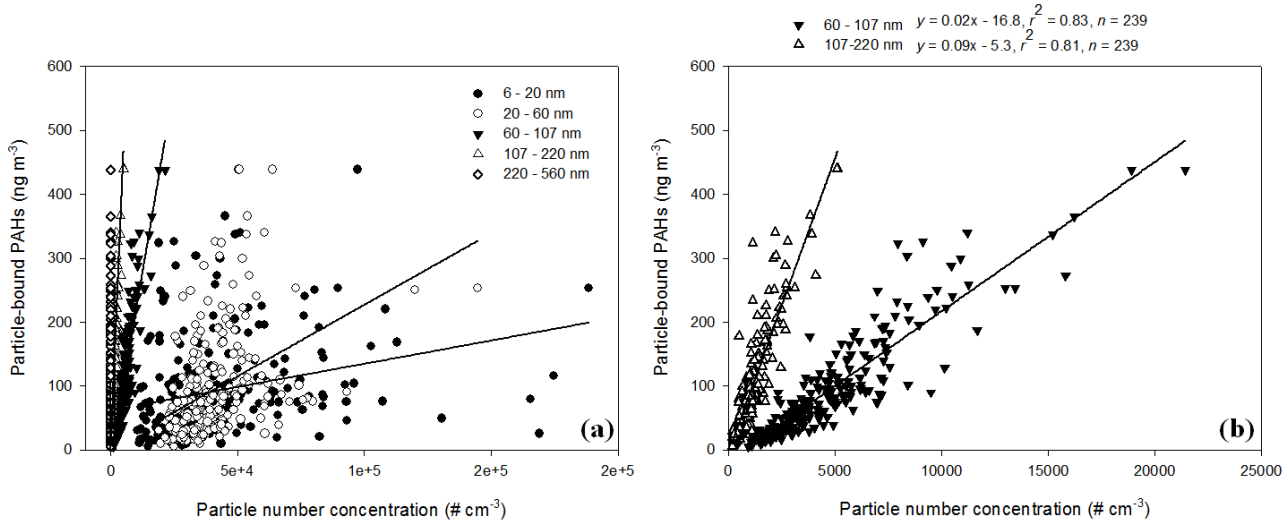

Fig. 4. Scatter plots of size-grouped particles vs. PM-PAHs from 60-s average concentrations on 22 December, 2011. (a) 6 < D_p < 560 nm, (b) 60 < D_p < 220 nm Size-grouped particles ●: 6 < D_p < 20 nm, ○: 20 < D_p < 60 nm, ▼: 60 < D_p < 107 nm, △: 107 < D_p < 220 nm, ◊: 6 < D_p < 220 nm (n = 239).

Table 6. Pearson's correlation (r^2) for 60-s average concentrations with different particle diameter (D_p) on 22 December 2011 (n = 239, p < 0.001 except for the number in bold).

	6 < D_p < 560 nm	6 < D_p < 20 nm	20 < D_p < 60 nm	60 < D_p < 107 nm	107 < Dp < 220 nm
BC	0.26	**0.19**	**0.18**	0.57	0.61
PM-PAHs	**0.16**	-	**0.17**	0.82	0.81
Surface area	0.46	0.25	0.52	0.78	0.70
CO_2	0.31	**0.19**	0.30	0.41	0.35
NO	0.36	0.29	0.30	**0.21**	**0.17**

the dominant contribution of diesel vehicles to emissions of relatively larger particles (60 < D_p < 220 nm) over the measurement period in our sampling area because PM-PAHs and BC are known to be emitted from diesel engines. Furthermore, as noted in the Introduction, the greater part of the particle number concentration from vehicle exhausts is in the 20–130 nm size range for diesel engines (Kittelson, 1998; Morawska *et al*., 1998) and in the 20–60 nm range for gasoline engines (Kittelson, 1998; Ristovski *et al*., 1998). Therefore, the linear relationships of the 60 < D_p < 220 nm particle size range with PAHs and BC indicate the dominance of diesel exhaust emissions for relatively larger particles in our study area, although it was difficult to determine the relative contributions of vehicle emissions for smaller particles (6 < D_p < 60 nm).

As Giechaskiel *et al*. (2005) observed, the nucleation mode is a particle size classification emitted by vehicles and consists fully of volatile compounds (Kittelson *et al*., 2006) whereas the non-volatile fraction accounts for the largest part of the soot particle mode (D_p > 50 nm). Baltensperger *et al*. (2002) and Wehner *et al*. (2004) observed a high non-volatile fraction for particles in the 80–150 nm size range, in ambient measurements with a high traffic influence. Kittelson *et al*. (2002, 2004a, b) conducted on-road measurements with two scanning mobility particle sizers (SMPS) equipped both with and without a thermal denuder (TD) operated at 300°C, to determine the non-volatile portion of the particle size distribution. They found that the TD removed between 87 and 95% of the particle number (nucleation mode) suggesting that most of the particles consisted of volatile material and that smaller particles were composed of more volatile materials. Similar

observations were also made by Weimer *et al.* (2009). In the present study, the $6 < D_p < 60$ nm particle size accounted for 93% of the total particle number concentrations, which is consistent with the findings of Kittelson *et al.* (2002, 2004a, b) and Weimer *et al.* (2009). Therefore, the nanoparticle ($D_p < 60$ nm) number concentrations in our study area may be related to volatile compounds, which can be emitted from either gasoline or diesel vehicles.

Time-Series Plots of Pollutants for Each Location

Figs. 5(a)–5(d) demonstrate very similar trends between UFP number concentrations and other associated pollutants. The 60-s average concentration data represent and summarize the trends of air pollutants better than the 1-s concentration data. Average concentrations of measured pollutants tended to be high in section [1] and low in section [2] for all measurements. The business district is located mainly in section [1] with dense residential areas in section [2]. Moreover, the sections differed in terms of number of road lanes, with up to 12 (8–12) lanes in section [1] and 4 lanes in section [2]. The large traffic volumes and the characteristics of section [1] (business district) may have contributed to the high concentrations of air pollutants. The region labeled as 1A in section [2], as shown in Figs. 5(a) through 5(d), indicates the measurement at the roadside background site. UFPs, particle surface area, and NO concentrations tend to show sharp concentration peaks over the first half of the distance driven in section [3], where a large interchange (Seocho I.C. of the Gyeongbu Expressway, the largest expressway in Korea) is located. The Seocho I.C. is located in the northwest of the study area and is about 500 m away from the locations sampled in first half of section [3]. The main wind directions during the measurement periods were northwest and west-northwest with an average wind speed of 3.2 ± 0.3 m/s (Korea Meteorological Administration). Hence, the sharp peaks in UFPs, particle surface area, and NO concentrations, labeled as 2A in Figs. 5 (a)–5(d), may have been generated by traffic at the Seocho I.C. Local wind speed plays an important role in determining the particle number size distributions in an urban area. Wu *et al.* (2008) observed that the nucleation ($3 < D_p < 20$ nm) and coarse mode ($D_p > 1$ μm) particle number concentrations

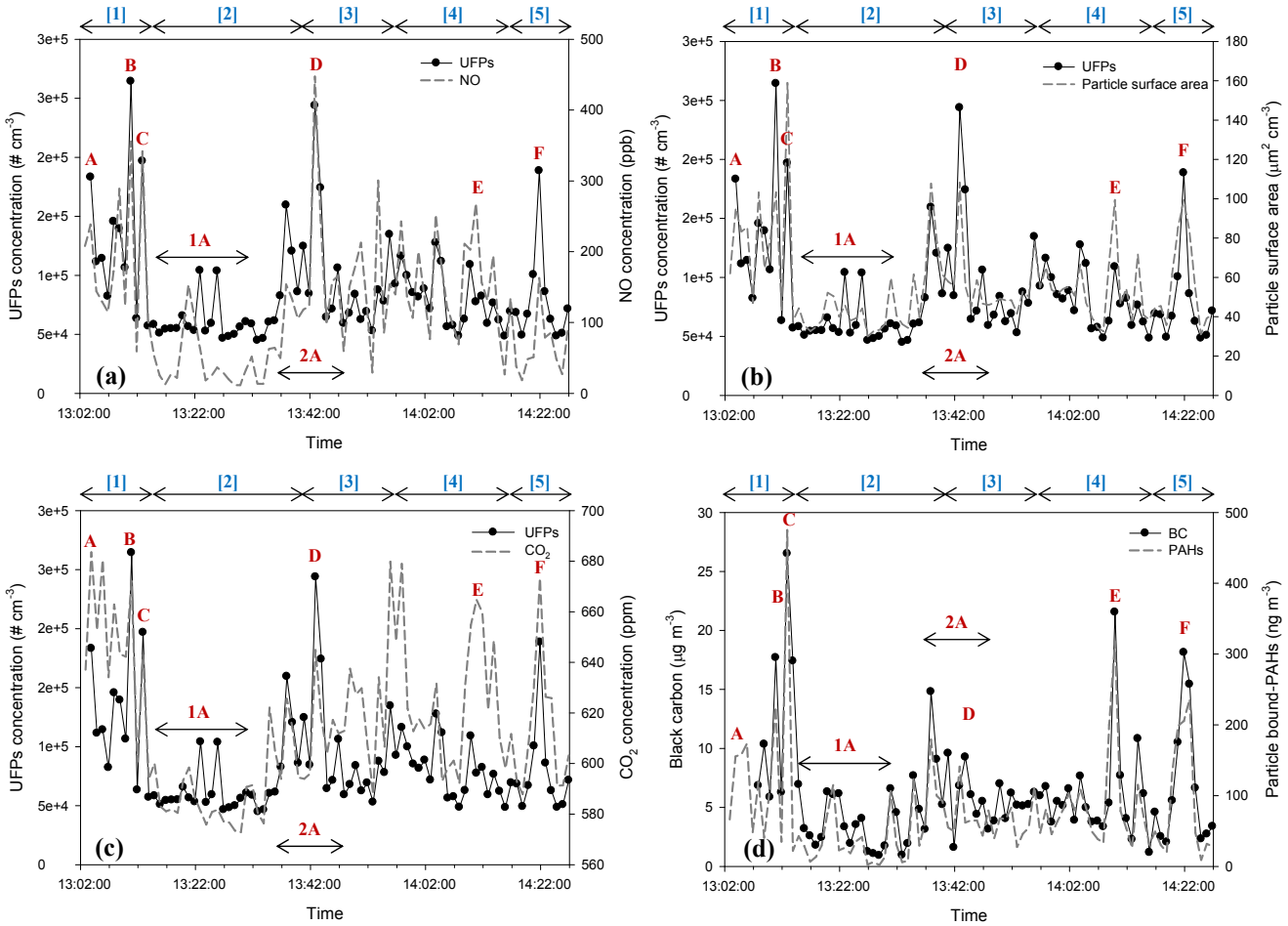

Fig. 5. Time-series plot of measured pollutants during 22 December arterial road ways. (a) UFPs total number vs. NO concentration, (b) UFPs total number vs. particle surface area (NAM), (c) UFPs total number vs. CO_2 concentration, (d) black carbon vs. PM-PAHs concentration ("A"–"F" indicates abundant peaks of pollutants; 1A indicates background measurement at roadside; 2A indicates sharp peaks of UFPs, particle surface area, and NO concentrations in the first half driving section [3].

increased, whereas the number concentrations of the Aitken mode ($20 < D_p < 100$ nm) and accumulation mode ($0.1 < D_p < 1$ μm) particles decreased with increasing wind speed in the urban area of Beijing. The observation of Wu *et al*. (2008) also supports the interpretation of sharp peaks observed for the region labeled 2A in Figs. 5 (a) and 5(b).

Several peaks of measured pollutants were observed across all the sections (A–F in Fig. 5). Interestingly, these peaks were commonly found at intersections reflecting the relationships of transient driving modes (i.e., deceleration and acceleration) with UFPs and associated pollutants (see Fig. 2, A–F indicated by blue circles). This is also related to the concentrated traffic volumes at intersections. Tong *et al*. (2000) previously reported that transient driving modes are more polluting than steady-speed driving modes (i.e., constant velocity) in terms of the pollutant amounts per distance (g/km) and time (g/s), although they measured only CO, HC, NO_x, and soot. They also observed that idling emissions of CO, HC, and NO_x were higher than those for acceleration and deceleration modes for both petrol and diesel vans in terms of fuel consumed (g/kg).

Comparisons with Other Studies

The UFP number concentrations and the concentrations of other pollutants measured in this study are compared with other studies in Table 7. Because only arterial roadways were studied in the present study, we compared the concentration levels observed on arterial roadways and background sites here. Note that the instruments may differ between studies, and the traffic volumes or other factors such as the condition of background sites must also be considered. For the roadway (not freeway) average, our study measured 97,000 particles/cm^3, whereas UFP concentrations of 40,000, 160,000, and 133,000 particles/cm^3 were reported by Westerdahl *et al*. (2005), Kittelson *et al*. (2004b), and Schneider *et al*. (2008), respectively. Our results are comparable to these previous findings, except those of Westerdahl *et al*. (2005). Our BC concentration was almost five times higher than that observed by Westerdahl *et al*. (2005), whereas we measured almost half the BC concentration observed by Schneider *et al*. (2008). Although PM-PAH concentrations were not reported by the studies carried out with a mobile platform shown in Table 7, roadside and on-road measurements taken with the same PM-PAH monitor (PAS 2000) in Mexico City showed up to 100–200 ng/m^3 (during morning rush hour) and 210–790 ng/m^3 of PM-PAHs, respectively (Marr *et al*., 2004, 2006). The concentrations of nitrogen oxides in our measurements were higher than those observed in the USA (Kittelson *et al*., 2004; Westerdahl *et al*., 2005). The background pollutant concentrations in our study also tended to be higher than those observed in other studies. However, it should be noted that our background area was located immediately beside the roadside in the center of an urban area in Seoul, whereas background sites for other studies were located outside urban areas.

UFP Numbers and Size Distributions

Overall, high particle number concentrations in the $6 < D_p < 20$ nm size range were measured in sections [1] and [4], while high particle number concentrations in the 60 <

Table 7. Comparison of reported average concentrations for UFPs and associated pollutants for roadways and background areas.

City (locations)	This study (2012) (Seoul, Korea)	Westerdahl *et al.* (2005) (Los Angeles, USA)	Kittelson *et al.* (2004a, b) (New York[c], Minnesota[d], USA)	Schneider *et al.* (2008) (Aachen, Germany)
Roadway average				
UFPs (1000 s/cm^3)		55–200 (F)[a]	200–560 (F)[c]	140 ± 48 (F)
	97 ± 18 (A)	40 (A)[b]	160 (A)[c]	133 ± 15 (A)
BC (μg/m^3)		2.4–20 (F)		3.2 ± 2.5 (F)
	7.4 ± 2.5 (A)	1.5 (A)		13.6 ± 3.2 (A)
PM-PAHs (ng/m^3)				
	98 ± 28 (A)			
NO_x (ppb)		230–470 (F)		
	203 ± 56 (A)	140 (A)		
NO (ppb)		120–470 (F)	100–240 (F)[c]	
	133 ± 33 (A)	79 (A)		
CO_2 (ppm)		800–900 (F)	400–420 (F)[c]	
	633 ± 12 (A)	720 (A)		
Background				
UFPs (1000 s/cm^3)	60 ± 29	14–27	9[d]	
BC (μg/m^3)	5.4 ± 0.6	0.4–1.6		1.5 ± 9.3
PM-PAHs (ng/m^3)	30.6 ± 46.4			
NO_x (ppb)	86 ± 67.4	35–50	15[d]	
NO (ppb)	51.6 ± 78.0	14–19		
CO_2 (ppb)	583.6 ± 10.2	368–475	364[d]	

[a] indicates "Freeway". [b] indicates "Arterial roadway", [c] indicates study in New York, [d] indicates study in Minnesota.
± indicates standard deviations of measured concentrations.

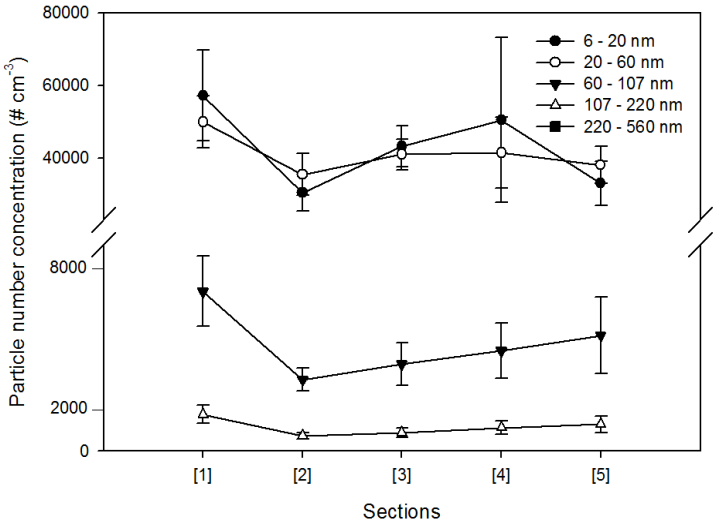

Fig. 6. Comparison of particle number concentration for five driving sections measured on December 22, 2011.

D_p < 220 nm size range were recorded in sections [1] and [5] (Fig. 6). The variations in BC and PM-PAH concentrations in the different sections were closely related to the particle numbers in the 60 < D_p < 220 nm size range and the number of road lanes and hence traffic volumes (Tables 2 and 3). Average vehicle speeds for sections [1], [2], [3], [4], and [5] were 17.4 ± 6.3, 12.5 ± 6.8, 16.7 ± 6.8, 11.1 ± 5.5, and 22.8 ± 8.0 km/h, respectively, indicating traffic congestion in section [4] when considering the number of road lanes available (see Table 2). Traffic congestion was frequently observed in section [4] due to the presence of shopping and entertainment areas and many crosswalks with traffic signals. The higher standard deviations recorded in section [4], particularly for the smaller particle size, strongly support this tendency. Large particles (60 < D_p < 220 nm) accounted for 7.4 and 8.0% of the total UFP number concentrations observed in sections [1] and [5], whereas in sections [2] to [4] the corresponding figures were 5.1 to 5.7%, as shown in Fig. 6. In summary, the relative contribution of smaller particles (6 < D_p < 60 nm) to the total measured was high in sections [2] to [4].

CONCLUSIONS

In the present study, we successfully measured UFPs and associated air pollutants using a mobile laboratory (ML). This study provides a link between roadside and vehicle emission measurements by estimating the spatial distributions of UFPs and associated air pollutants, on real-world roadways, to enhance understanding of traffic emissions and characterize pollution gradients along roadways.

High determination coefficients (r^2 = 0.65) among the pollutants associated with diesel vehicles (BC and PM-PAHs) indicate the influence of diesel vehicles in our study area. Although poor correlations between total UFP number concentrations and BC or PM-PAHs were recorded, size-classified larger particles ranging from 60 < D_p < 220 nm showed much higher determination coefficients with PM-PAHs and BC concentrations whereas poor correlations were recorded for the size-classified smaller particles ranging from 6 < D_p < 60 nm with PM-PAHs and BC concentrations. The higher correlations of UFP number concentrations for the 60 < D_p < 220 nm size range with PM-PAHs, BC, and particle surface area strongly reflect the dominant contribution of diesel vehicle exhaust emissions for relatively larger particles (60 < D_p < 220 nm) over the measurement period in our monitoring area. Several peaks of measured pollutants were observed, mostly at intersections, reflecting the relationships of transient driving modes (i.e., deceleration and acceleration) with UFPs, associated pollutants, and concentrated traffic volumes.

ACKNOWLEDGEMENTS

This study was supported in part by the Center for Environmentally Friendly Vehicles and the KIST (Korea Institute of Science and Technology) Institutional Program (2E24651).

SUPPLEMENTARY MATERIALS

Supplementary data associated with this article can be found in the online version at http://www.aaqr.org.

REFERENCES

Baltensperger, U., Streit, N., Weingartner, E., Nyeki, S., Prévôt, A.S.H., van Dingenen, R., Virkkula, A., Putaud, J.P., Even, A., ten Brink, H., Blatter, A., Neftel, A. and Gäggeler, H.W. (2002). Urban and Rural Aerosol Characterization of Summer Smog Events during the PIPAPO Field Campaign in Milan, Italy. *J. Geophys. Res*. 107: 8193, doi: 10.1029/2001JD001292.

Bukowiecki, N., Kittelson, D.B., Watts, W.F., Burtscher, H., Weingartner, E. and Baltensperger, U. (2002a). Real-Time Characterization of Ultrafine and Accumulation Mode Particles in Ambient Combustion Aerosols. *J. Aerosol Sci.* 33: 1139–1154.

Bukowiecki, N., Dommen, J., Prévôt, A.S.H., Richter, R., Weingartner, E. and Baltensperger, U. (2002b). A Mobile Pollutant Measurement Laboratory-measureing Gas Phase and Aerosol Ambient Concentrations with High Spatial and Temporal Resolution. *Atmos. Environ.* 36: 5569–5579.

Buoanno, G., Lall, A.A. and Stabile, L. (2009). Temporal Size Distribution and Concentration of Particles near a Major Highway. *Atmos. Environ.* 43: 1100–1105.

Burtscher, M. (1992). Measurement and Characteristics of Combustion Aerosols with Special Consideration of Photoelectric Charging and Charging by Flame Ions. *J. Aerosol Sci.* 23: 549–595.

Canagaratna, M.R., Jayne, J.T., Ghertner, D.A., Herndon, S., Shi, Q., Jimenez, J.L., Silva, P.J., Williams, P., Lanni, T., Drewnick, F., Demerjian, K.L., Kolb, C.E. and Worsnop, D.R. (2004). Chase Studies of Particulate Emissions from In-use New York City Vehicles. *Aerosol Sci. Technol.* 38: 555–573.

Cass, G.R., Hughes, L.A., Bhave, P., Kleeman, M.J., Allen, J.O. and Salmon, L.G. (2000). The Chemical Composition of Atmospheric Ultrafine Particles. *Philos. Trans. R. Soc. London, Ser. B* 358: 2581–2592.

Dunbar, J.C., Lin, C.I., Vergucht, I., Wong, J. and Durant, J.L. (2001). Estimating the Contributions of Mobile Sources of PAH to Urban Air Using Real-time PAH Monitoring. *Sci. Total Environ.* 279: 1–19.

EPA (2000). National Air Pollution Emission Trends 1900-1998, 1998 Emissions. United States Environmental Protection Agency.

Giechaskiel, B., Ntziachristos, L., Samaras, Z., Scheer, V., Casati, R. and Vogt, R. (2005). Formation Potential of Vehicle Exhaust Nucleation Mode Particles On-road and in the Laboratory. *Atmos. Environ.* 39: 3191–3198.

Hagler, G.S.W., Baldauf, R.W., Thoma, E.D., Long, T.R., Snow, R.F., Kinsey, J.S., Oudejans, L. and Gullett, B.K. (2009). Ultrafine Particles near a Major Roadway in Raleigh, North Carolina: Downwind Attenuation and Correlation with Traffic Related Pollutants. *Atmos. Environ.* 43: 1229–1234.

Harrison, R.M., Shi, J.P., Xi, S.H., Khan, A., Mark, D., Kinnersley, R. and Yin, J.X. (2000). Measurement of Number, Mass and Size Distribution of Particles in the Atmosphere. *Philos. Trans. R. Soc. London, Ser. A* 358: 2567–2579.

Hitchins, J., Morawska, L., Wolff, R. and Gilbert, D. (2000). Concentrations of Submicrometre Particles from Vehicle Emissions near a Major Road. *Atmos. Environ.* 34: 51–59.

Kim, K.H., Sekiguchi, K., Kudo, S. and Sakamoto, K. (2011a). Characteristics of Atmospheric Elemental Carbon (Char and Soot) in Ultrafine and Fine Particles in a Roadside Environment, Japan. *Aerosol Air Qual. Res.* 11: 1–12.

Kim, K.H., Sekiguchi, K., Furuuchi, M. and Sakamoto, K. (2011b). Seasonal Variation of Carbonaceous and Ionic Components in Ultrafine and Fine Particles in an Urban Area of Japan. *Atmos. Environ.* 45: 1581–1590.

Kim, K.H., Sekiguchi, K., Kudo, S., Kinoshita, M. and Sakamoto, K. (2013). Carbonaceous and Ionic Components in Ultrafine and Fine Particles at Four Sampling Sites in the Vicinity of Roadway Intersection. *Atmos. Environ.* 74: 83–92.

Kittelson, D.B. (1998). Engines and Nanoparticles: A Review. *J. Aerosol Sci.* 29: 575–588.

Kittelson, D.B., Watts, W.F. and Johnson, J.P. (2002). Diesel Aerosol Sampling Methodology-CRC-43 Final Report, Alpharetta, GA: Coordinating Research Council, Available at http://www.crcao.com/.

Kittelson, D.B., Watts, W.F., Johnson, J.P., Remerowki, M.L., Ische, E.E., Oberdörster, G., Gelein, R.M., Elder, A., Hopke, P.K., Kim, E., Zhao, W. and Jeong, C.H. (2004a). On-road Exposure to Highway Aerosols 1: Aerosol and Gas Measurements. *Inhalation Toxicol.* 16: 31–39.

Kittelson, D.B., Watts, W.F. and Johnson, J.P. (2004b). Nanoparticle Emissions on Minnesota Highways. *Atmos. Environ.* 38: 9–19.

Kittelson, D.B., Watts, W.F. and Johnson, J.P. (2006). On-road and Laboratory Evaluation of Combustion Aerosols – Part 1: Summary of Diesel Engine Results. *J. Aerosol Sci.* 37: 913–930.

Marr, L.C., Grogan, L.A., Wohrnschimmel, H., Molina, L.T., Molina, M.J. and Garshick, E. (2004). Vehicle Traffic as a source of Particulate Polycyclic Aromatic Hydrocarbon Exposure in the Mexico City Metropolitan Area. *Environ. Sci. Technol.* 38: 2584–2592.

Marr, L.C., Dzepina, K., Jimenez, J.L., Reisen, F., Bethel, H.L., Arey, J., Gaffney, J.S., Marley, N.A., Molina, L.T. and Molina, M.J. (2006). Sources and Transformations of Particle-bound Polycyclic Aromatic Hydrocarbons in Mexico City. *Atmos. Chem. Phys.* 6: 1733–1745.

Ministry of Environment (2009). Basis Construction of Nano-PM Evaluation & Management 33-1-0-04. Ministry of Environment, Republic of Korea.

Morawska, L., Bofinger, N.D., Kocis, L. and Nwankwoala, A. (1998). Submicrometer and Supermicrometer Particles from Diesel Vehicle Emissions. *Environ. Sci. Technol.* 32: 2033–2042.

Morawska, L., Ristovski, Z., Jayaratne, E.R., Keogh, D.U. and Ling, X. (2008). Ambient Nano and Ultrafine Particles from Motor Vehicle Emissions: Characteristics, Ambient Processing and Implications on Human Exposure. *Atmos. Environ.* 42: 8113–8138.

Pirjola, L., Parviainen, H., Hussein, T., Valli, A., Hämeri, K., Aaalto, P., Virtanen, A., Keskinen, J., Pakkanen, T.A., Mäkelä, T. and Hillamo, R.E. (2004). "Sniffer"- A Novel Tool for Chasing Vehicles and Measuring Traffic Pollutants. *Atmos. Environ.* 38: 3625–3635.

Polidori, A., Hu, A., Biswas, S., Delfino, R.J. and Sioutas, C. (2008). Real-time Characterization of Particle-bound Polycyclic Aromatic Hydrocarbons in Ambient Aerosols and from Motor-vehicle Exhaust. *Atmos. Chem. Phys.* 8: 1277–1291.

Ristovski, Z., Morawska, L., Bofinger, N.D. and Hitchins, J. (1998). Submicrometer and Supermicrometer Particles from Spark Ignition Vehicle Emissions. *Environ. Sci. Technol.* 32: 3845–3852.

Schauer, J.J., Rogge, W.F., Hildemann, L.M., Mazurek,

M.A., Cass, G.R. and Simoneit, B.R.T. (1996). Source Apportionment of Airborne Particulate Matter Using Organic Compounds as Tracers. *Atmos. Environ.* 30: 3837–3855.

Schneider, J., Kirchner, U., Norrmann, S., Vogt, R. and Scheer, V. (2008). In Situ Measurements of Particle Number Concentration, Chemically Resolved Size Distributions and Black Carbon Content of Traffic-related Emissions on German Motorways, Rural Roads and in City Traffic. *Atmos. Environ.* 42: 4257–4268.

Shi, J.P., Khan, A.A. and Harrison, R.M. (1999). Measurements of Ultrafine Particle Concentration and Size Distribution in the Urban Atmosphere. *Sci. Total Environ.* 235: 51–64.

Statistics Korea (2011). Registered Motor Vehicles and Trend, Statistics Korea.

Tong, H.Y., Hung, W.T. and Cheung, C.S. (2000). On-road Motor Vehicle Emissions and Fuel Consumption in Urban Driving Conditions. *J. Air Waste Manage. Assoc.* 50: 543–554.

Venkataraman, C. and Friedlander, S.K. (1994). Size Distributions of Polycyclic Aromatic Hydrocarbon and Elemental Carbon 2: Ambient Measurements and Effects of Atmospheric Processes. *Environ. Sci. Technol.* 28: 563–572.

Wang, M., Zhu, T., Zheng, J., Zhang, R.Y., Zhang, S.Q., Xie, X.X., Han, Y.Q. and Li, Y. (2009). Use of a Mobile Laboratory to Evaluate Changes in On-road Air Pollutants during the Beijing 2008 Summer Olympics. *Atmos. Chem. Phys.* 9: 8247–8263.

Wehner, B., Philippin, S., Wiedensohler, A., Scheer, V. and Vogt, R. (2004). Variability of Non-volatile Fractions of Atmospheric Aerosol Particles with Traffic Influence. *Atmos. Environ.* 38: 6081–6090.

Weijers, E.P., Khlystov, A.Y., Kos, G.P.A. and Erisman J.W. (2004). Variability of Particulate Matter Concentrations along Roads and Motorways Determined by a Moving Measurement Unit. *Atmos. Environ.* 38: 2993–3002.

Weimer, S., Mohr, C., Richter, R., Keller, J., Mohr, M., Prévôt, A.S.H. and Baltensperger, U. (2009). Mobile Measurements of Aerosol Number and Volume Size Distributions in an Alpine Valley: Influence of Traffic versus Wood Burning. *Atmos. Environ.* 43: 624–630.

Westerdahl, D., Fruin, S., Sax, T., Fine, P.M. and Sioutas, C. (2005). Mobile Platform Measurements of Ultrafine Particles and Associated Pollutants Concentrations on Freeways and Residential Streets in Los Angeles. *Atmos. Environ.* 39: 3597–3610.

Wu, Z., Hu, M., Lin, P., Liu, S., Wehner, B. and Wiedensohler, A. (2008). Particle Number Size Distribution in Urban Atmosphere of Beijing, China. *Atmos. Environ.* 42: 7967–7980.

Zhu, Y.F., Hinds, W.C., Kim, S., Shen, S. and Sioutas, C. (2002a). Study of Ultrafine Particles near a Major Highway with Heavy-duty Diesel Traffic. *Atmos. Environ.* 36: 4323–4335.

Zhu, Y.F., Hinds, W.C., Kim, S. and Sioutas, C. (2002b). Concentration and Size Distribution of Ultrafine Particles near a Major Highway. *J. Air Waste Manage. Assoc.* 52: 1032–1042.

Received for review, January 17, 2014
Revised, March 4, 2014
Accepted, April 9, 2014

Supplementary Materials

On-Road Measurements of Ultrafine Particles and Associated Air Pollutants in a Densely Populated Area of Seoul, Korea

Kyung Hwan Kim[1], Daekwang Woo[1, 2], Seung-Bok Lee[1], Gwi-Nam Bae[1*]

Traffic volume and composition of vehicles within the same measurement area in Gangnam, Seoul measured in 2012 are shown in Table S1. Traffic volume and composition was measured with the image provided by Seoul Metropolitan Police Agency.

Table S1. Traffic composition and volume of main streets of Gangnam measured in November 2012.

Main streets of Gangnam	Bike	LPG	Gasoline	Diesel	Traffic volume (vehicles/h)	Lane
Samseong	5.3%	19.9%	43.5%	31.3%	7608	14
Nonhyun	7.4%	22.1%	38.5%	31.9%	4960	10
Dosan	6.0%	18.0%	46.7%	29.4%	4968	8
Gangnam	8.4%	24.8%	35.9%	30.8%	5232	10
Youngdong	0.0%	14.5%	50.3%	35.2%	11540	8
Mean (±σ)	5.4±3.3%	19.9±3.9%	43.0±5.9%	31.7±2.1%	6862±2842	10±2

Mean traffic composition shows vehicles powered by gasoline, diesel, and liquefied petroleum gas (LPG) accounting for 48.4, 31.7, and 19.9% of the total, respectively which is somewhat similar with the vehicle composition provided Statistics Korea in 2011 (gasoline: 49.7%, diesel: 36.4%, and LPG: 13.2%).

However, the traffic composition was estimated by visual inspection thus, there would be differences especially for the passenger car. Despite the temporal spatial difference of measurement, overall traffic composition data showed quite similar vehicle composition with those provided by

Statistics Korea in 2011 reflecting that traffic composition does not show significant spatial and temporal changes. The traffic volume indicates that Gangnam area is a heavy traffic area.